

# Unbiased Determination of Absolute Configurations by vis-à-vis Comparison of Experimental and Simulated Spectra: The Challenging Case of Diplopyrone

*Marco Fusè,<sup>†,#</sup> Giuseppe Mazzeo,<sup>¶,#</sup> Giovanna Longhi,<sup>¶,§</sup> Sergio Abbate,<sup>\*,¶,§</sup> Marco Masi,<sup>‡</sup>*

*Antonio Evidente,<sup>\*,‡</sup> Cristina Puzzarini,<sup>&</sup> Vincenzo Barone,<sup>\*,†</sup>*

<sup>†</sup> Scuola Normale Superiore, Piazza dei Cavalieri 7, I-56126 Pisa, Italy

<sup>‡</sup> Dipartimento di Scienze Chimiche, Università di Napoli Federico II, Complesso Universitario  
Monte S. Angelo, Via Cintia 4, 80126 Napoli, Italy

<sup>&</sup> Dipartimento di Chimica “Giacomo Ciamician”, Università di Bologna, Via Selmi 2, I-40126  
Bologna, Italy

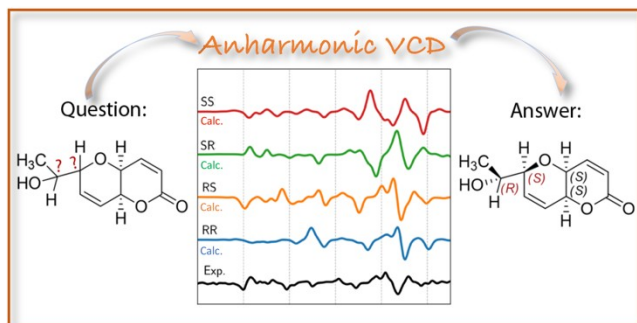
<sup>¶</sup> Dipartimento di Medicina Molecolare e Traslazionale, Università di Brescia, Viale Europa 11,  
25123 Brescia, Italy

<sup>§</sup> Consiglio Nazionale delle Ricerche-I.N.O. c/o CSMT via Branze, 45 – 25123 Brescia, Italy

<sup>#</sup> **These authors contributed equally to this work.**

[ABSTRACT] A new experimental-computational strategy for the determination of the absolute configuration (AC) of complex chiral molecules is proposed by combining diverse experimental spectroscopies with quantum-mechanical simulations well beyond the current computational practice. Key features are the conformer search and relative stability evaluation performed by a new stochastic two-level tool followed by a vis-à-vis comparison of experimental and computed spectra without any ad hoc adjustment. The entire computational procedure is embedded in the user-friendly VMS software and its reliability is granted by the inclusion of mechanic/electric/magnetic anharmonicity as well as ro-vibrational and vibronic couplings by means of generalized perturbation theory in conjunction with double-hybrid functionals combined with empirical dispersion contributions and suitable basis sets. To test and validate the new approach, the puzzling case of diplopyrone, a phytotoxic metabolite, has been chosen: the close match between new experimental and simulated IR and VCD spectra has led to the unbiased evaluation of its AC.

## TOC GRAPHICS



## 1. Introduction

The knowledge of the absolute configuration (AC) is a fundamental milestone in the proper characterization of newly synthesized chiral molecules, but also of – synthetic or natural – chiral compounds already in use. However, when the molecular complexity is such that more than 1-2 chiral centers and several low-energy conformers are concomitantly present, the determination of AC is not straightforward at all and becomes, instead, a great challenge.

On this ground lies the importance of developing a reliable and effective strategy to unequivocally determine the AC of a chiral molecule irrespective of its size and complexity. Infrared absorption and vibrational circular dichroism spectroscopies (IR, VCD) are emerging as the spectroscopic techniques of choice for this strategy<sup>1-4</sup> in view of their improved sensitivity and reliability with respect to the more standard circular dichroism (CD) technique in the UV-visible range (nowadays denoted as electronic CD, ECD)<sup>5</sup> and even – sometimes – to the ultimate method for structure determination, namely X-Ray diffraction.<sup>6</sup>

An unbiased discrimination among different AC hypotheses generally requires several spectroscopic techniques combined with powerful computational tools in order to exploit a quantitative comparison of experimental and simulated spectra.<sup>7-9</sup> Indeed, judging whether calculated spectra associated with one AC choice are better than those based on other AC choices cannot be solely based on visual qualitative comparison or on mere numbers; instead, an approach based on quantitative comparisons of spectra, possibly exploiting statistical methods,<sup>10-13</sup> is required. To reach this goal, we resort to the virtual multi-frequency spectrometer (VMS) project,<sup>14</sup> which allows a direct *vis-à-vis* comparison between in vitro and in silico experiments for a large panel of spectroscopies without any arbitrariness thanks to a user-friendly access to state-of-the-art computational approaches in combination with advanced graphical tools.

One strong limitation that still affects computational spectroscopy is to often rely on oversimplified models (e.g. vertical excitation, harmonic oscillator, rigid rotor), which require the introduction of ad-hoc corrections (e.g. scaling factors, somehow accounting for mechanical anharmonicity<sup>15</sup>). As a matter of fact, more advanced (e.g. anharmonic and/or vibronic) models<sup>7</sup> are usually employed only by theoretically-oriented groups or to deal with some specific cases for which they cannot be avoided, such as the analysis of portions of vibrational spectra (especially in the near infrared, NIR)<sup>16,17</sup> obtained with medium-to-high resolution experiments in the gas phase or in inert matrices and/or for resonant regimes (Resonance-Raman and its chiral RROA counterpart).<sup>7,14,18-22</sup> The situation is even more involved when electric and/or magnetic anharmonicity come into play: for instance, in vibrational spectroscopies the intensity of overtones and/or combination bands vanishes at the harmonic level. Thanks to ongoing developments, the computational efficiency and robustness of vibronic models and second-order vibrational perturbation theory (VPT2)<sup>7,23,24</sup> are becoming more routinely available to provide spectra that do not require any additional empirical correction. However, two specific issues have to be addressed in order to achieve reliable results, namely the presence of large amplitude motions (LAMs) and of resonances between nearly degenerate states. These two issues are discussed in some detail in the Computational Details section with special reference to vibrational spectroscopies; here, we only anticipate that our vibronic and generalized VPT2 (GVPT2) models<sup>7</sup> have been further extended to allow a fully automatic treatment of weakly coupled LAMs and resonances, also including those plaguing the computation of intensities, which are by no means standard.

On these grounds, we introduce an effective strategy to determine the AC of chiral molecules based on a direct *vis-à-vis* comparison of experimental and computed spectra, the latter being

obtained by second-order expansions of mechanic, electric and magnetic anharmonicity, together with ro-vibrational and, possibly, vibronic couplings.

To present and validate the key steps of our general strategy, we make use of a specific example: the challenging case of the AC of diplopyrone, a compound with four stereocenters and thus a total of  $2^4 = 16$  diastereoisomers (see **Figure 1**), which allows us to demonstrate the reliability of our approach.

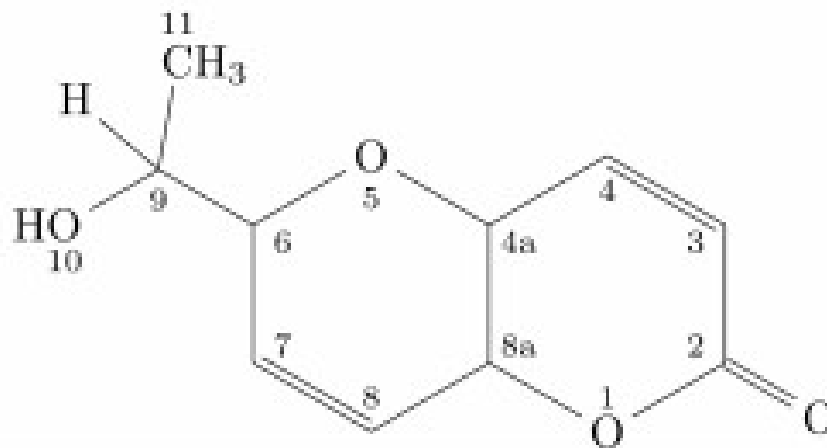


**Figure 1.** Chemical Structure and relevant atom numbering of diplopyrone (**1**).

Diplopyrone (**1**) is a phytotoxic metabolite of *Diplodia corticola*, also previously isolated from *Diplodia mutila*. Both of them are phytopathogenic fungi causing different forms of cork oak canker on *Quercus suber*, with heavy economic losses.<sup>35,36</sup> The structure of **1** was first determined by spectroscopic methods and the AC of the chiral secondary hydroxylated carbon (C-9) was assigned as (*S*)<sup>37</sup> by applying Mosher's method.<sup>38</sup> Later, after an extensive NMR analysis, the AC of **1** was determined as 4a(*S*), 6(*R*), 8a(*S*), based on the combination of two different methods: (a) the exciton analysis of the CD spectrum and (b) the DFT calculation of the optical rotatory power.<sup>39</sup> A deeper inspection of the available spectroscopic data, also

reconsidering the performance of the instrumentation employed, led us to conclude that the AC assignment was correct for centers 4a(*S*) and 8a(*S*), with ECD and NMR providing coincidental answers, while the C-9 and C-6 centers need a careful re-consideration, in agreement with the analysis of ref. 39, recently reporting the asymmetric synthesis of **1**.

## 2. Experimental Details

VCD spectra were obtained using a Jasco FVS6000 FTIR apparatus equipped with wire grid polarizer, ZnSe photoelastic modulator, and MCT detector; 200  $\mu\text{m}$  BaF<sub>2</sub>-cells were employed, filled with 0.1 M concentrated solutions in CDCl<sub>3</sub>. Spectra were obtained by averaging 5000 scans. For both IR and VCD spectra, solvent subtraction was performed.

## 3. Computational Details

The underlying electronic-structure model is rooted in the density functional theory (DFT) and its time-dependent extension (TD-DFT). Hybrid (B3LYP<sup>25</sup>) and double-hybrid (B2PLYP<sup>26,27</sup>) models, augmented by empirical dispersion contributions (here Grimme's D3 model<sup>28</sup>), in conjunction with medium-sized basis sets including diffuse functions (the jun-cc-pVnZ<sup>29,30</sup> family of basis sets, with n=D,T) have been employed. To select low-energy structures, a powerful stochastic two-stage search tool,<sup>31</sup> also taking into account solvent effects by means of the polarizable continuum model (PCM),<sup>32</sup> has been used. Noted is that this model is fully adequate for 'innocent' solvents (like CDCl<sub>3</sub>, employed in this study), whereas the situation is more involved for hydrogen-bonding solvents, whose treatment requires more sophisticated discrete-continuum models coupled to molecular dynamics (or Monte Carlo) approaches.<sup>33,34</sup>

However, we do not deal with these situations in the present study, this supporting the suitability of PCM.

All computations have been performed by integrated scripts mostly governed by the VMS software<sup>14</sup> and its interface to the Gaussian suite of programs.<sup>40</sup> Geometry optimizations were carried out employing very tight convergence criteria and minima were confirmed by Hessian evaluations. Harmonic force fields were obtained using analytic derivatives of energy, while transition moments and higher-order derivatives were computed through numerical differentiation using a step of  $0.01 \text{ amu}^{1/2} \text{a}_0$  for the displacements along the mass-weighted normal coordinates. Free energies in the gas-phase were determined by adding zero-point energy and thermal contributions, both evaluated in the framework of the rigid rotor / harmonic oscillator approximation, to electronic energies. As far as PCM contributions are concerned, they already have the “status” of free energies.<sup>32</sup>

### **3.1. Anharmonic calculations**

As mentioned in the Introduction, the GVPT2 approach was used for the resolution of the nuclear problem. The anharmonic treatment was obtained by combining VPT2 with semi-diagonal fourth-order expansions of potential energy surfaces and third-order semi-diagonal representations of the property surfaces. However, as already pointed out, the VPT2 treatment is strongly affected by the presence of LAMs and/or resonances.

LAMs are not only poorly described by VPT2, but they can also contaminate its results, thus leading to large errors on those vibrations that are coupled to LAMs, even if intense and at high frequency. Therefore, their identification and exclusion (together with all their anharmonicity constants) from the VPT2 treatment are required to achieve reliable results. LAMs are generally connected to torsions and inversion motions. In the present systems, the low energy modes

associated to the torsion angle between the two fused rings, the rotation of the methyl and exocyclic carbinol groups, and the out-of-plane bending of the OH group have been removed (a complete list of the removed normal modes for each anharmonic calculation is provided in the Supporting Information, SI). Provided that the couplings of LAMs among themselves and with other vibrational modes are weak, they can be effectively treated by variational or quasi-variational approaches whenever (contrary to the present case) low-frequency regions of the spectra are of interest.<sup>7</sup>

The second issue that plagues VTP2 calculations is the presence of resonances. In this work, we have relied on the so-called GVPT2 method, in which diverging terms in the perturbative expression are removed from the perturbative summations (DVPT2) and resonances are treated in a second step with a reduced-dimensionality variational calculation (GVPT2), Fermi (FRs) and Darling-Dennison resonances (DDRs) being identified through two-step procedures and treated as described in references 7,18,23 (some details are also provided in the SI).

In addition to the default tests for the identification of resonances implemented in the Gaussian suite of programs,<sup>18,23,24,40</sup> we have here introduced a specific two-step procedure to identify resonances affecting only intensities. Since FRs cause intensity redistribution between 1-quantum and 2-quanta transitions, the test is indeed inspired to the expression of the transition moments for a 2-quanta transition,  $\langle P \rangle_{0,(1+\delta_{ji})(1-\delta_{ji})}$ :

$$\langle P \rangle_{0,(1+\delta_{ji})(1-\delta_{ji})} = \frac{1}{2(1+\delta_{ij})_i} \left[ P_{i,j} + \sum_{k=1}^N k_{ijk} P_k \left( \frac{1}{\omega_i + \omega_j - \omega_k} - \frac{1}{\omega_i + \omega_j + \omega_k} \right) \right]$$

In the expression above,  $\frac{k_{ijk} P_k}{\omega_i + \omega_j - \omega_k}$  represents the only possibly divergent term, and it can be used to recognize potentially problematic situations. The first step of the procedure is a test

performed on the frequency difference ( $|\Delta\omega|$ ), which is then followed by a second test based on the ratio between the property of interest  $P_k$  and  $\Delta\omega$  ( $P_k^2/|\Delta\omega|$ ):

$$\text{Step 1: } |\Delta\omega| \leq \Delta_{\omega_i}^{1-2} \quad \text{Step 2: } \frac{P_k^2}{|\Delta\omega|} \geq K_I^{1-2}$$

where  $\Delta_{\omega_i}^{1-2}$  and  $K_I^{1-2}$  are the intensity specific threshold values. Since the  $k_{ijk}$  force constants are unknown at the harmonic level, the property itself is used as an excess approximation.

A shortcoming of this approach is that, in principle, a different test with a specific threshold is required for each investigated property. On the other hand, the strength of this approach is that it can be performed without any additional computational cost on all the properties already available at the harmonic level of theory. In this work, this two-step procedure has been employed on the dipole and rotatory strengths of different transitions in order to account the presence of FRs for both IR and VCD spectra (a complete list of the threshold employed in anharmonic calculations is provided in SI).

#### 4. Results and Discussion

Our general strategy, which involves three steps, is presented in the following and discussed in its application to the diplopyrone test case.

*1. Generation of low-lying conformers.* As briefly mentioned above, we employed a recently proposed two-stage stochastic procedure<sup>31</sup> interfaced to VMS<sup>14</sup> and the Gaussian suite of programs,<sup>40</sup> thus giving access to all quantum-mechanical (QM), molecular mechanics (MM) and hybrid models available in the latter code. In our approach, a large set of structures is first generated by a sampling of dihedral angles (or, if needed, other soft degrees of freedom<sup>41</sup>) using a fast MM or semiempirical QM method (here the MMFF94s force field<sup>42</sup>). Then, their energy is

re-evaluated using B3LYP-D3<sup>25,28</sup> in conjunction with a medium-sized basis set (here TZVP<sup>43</sup>). Finally, the geometries of the most promising candidates are fully optimized at the latter level of theory to obtain a short-list of representative low-lying conformers.

Several tests have shown that this integrated approach represents a very good compromise between accuracy and computational cost. In the case of **1**, the initial search provided (within a very conservative window of 80 kJ mol<sup>-1</sup>) 19 conformers for the *S-R-SS* AC choice, 13 for *S-S-SS*, 18 for *R-R-SS* and 14 for *R-S-SS* (by convention, the order of chiral centers is 9, 6, 4a, 8a; see **Figure 1** for atom numbering). After full geometry optimizations at the PCM/B3LYP-D3/TZVP level of all these structures, the five most stable conformers of each diastereoisomer have been selected for further consideration. For three diastereoisomers, this choice covers more than 90% of the relative population at room temperature (see Table S1 of the SI). However, for *S-R-SS* the lower hindrance between the substituent in 6 and the lactone rings makes accessible two half-chair conformations on the ether ring, thus increasing the number of low-energy conformers. Since this diastereoisomer is – anyway – relatively unstable, an accurate description of all its conformers is not required (*vide infra*).

2. *Evaluation of relative stabilities and Boltzmann populations.* In a second step, taking the advantage of previous studies,<sup>44,45</sup> we resorted to the B3LYP-D3/jun-cc-pVDZ<sup>25,28,29</sup> (hereafter B3) and B2PLYP-D3/jun-cc-pVTZ<sup>26-29</sup> (hereafter B2) models for computing the relative stabilities of low-energy diastereoisomers and conformers. Note that, inclusion of diffuse functions is mandatory to accurately describe non-covalent interactions<sup>30</sup> and the jun-family basis sets provide results very close to the parent fully augmented basis sets at a significantly reduced cost.

This step is critical since the final simulated spectrum can be very sensitive to the Boltzmann population of different low-energy structures. It has been recently claimed that standard hybrid functionals and basis sets are not accurate enough to this end and that refinement of conformer populations, in order to optimize the agreement between computed and experimental spectra, leads to improved results.<sup>46</sup> However, we refrain from this choice because it introduces an unwanted degree of empiricism and could impair unbiased interpretation of the results with the risk of obtaining ‘good results for the wrong reason’. To give further support to our strategy, we have performed an exhaustive conformer search and energy evaluation for the serine aminoacid in gas phase for which very accurate results,<sup>47</sup> obtained by the so-called focal point analysis (FPA),<sup>48</sup> are available. For comparison purposes, together with hybrid and double-hybrid functionals we have also considered second-order Moller-Plesset perturbation theory (MP2),<sup>49</sup> which is often employed in energetics evaluations.

**Table 1.** Relative stabilities of serine conformers (see ref. 47 for definition and labeling) and errors with respect to FPA computations in kJ mol<sup>-1</sup>.

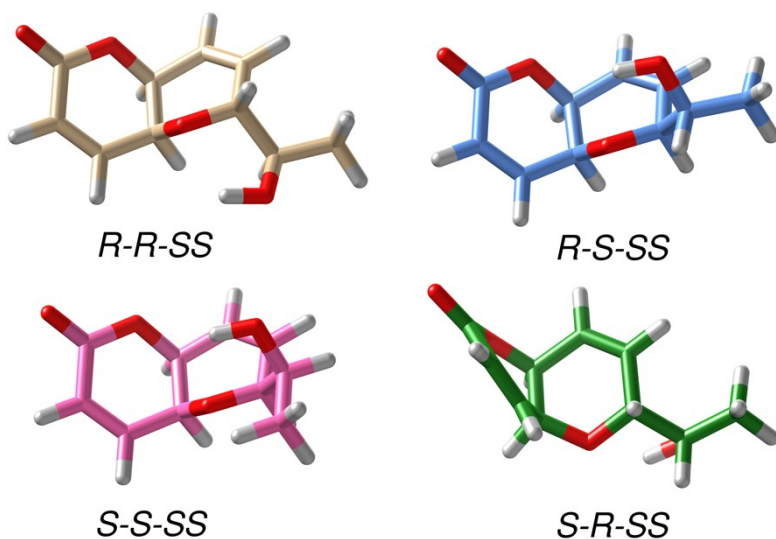
Conformer	B3	MP2/jTZ <sup>a</sup>	B2	FPA <sup>b</sup>
TT1	0.0	0.0	0.0	0.0
CC1	1.21	2.22	1.63	2.09
TT2	0.60	3.52	2.10	2.68
CC2	5.14	3.61	4.01	3.56
CA1	6.76	7.14	6.30	6.02
TT3	7.56	6.69	7.00	7.57
CA2	9.74	10.59	9.39	9.37
Abs. err.	0.94	0.71	0.39	
Max. err.	2.08	1.22	0.58	

<sup>a</sup> MP2 calculations in conjunction with the jun-cc-pVTZ basis set. <sup>b</sup> From ref. 47: FPA performed at MP2/aug-cc-pVTZ geometries, which are nearly identical to MP2/jun-TZ geometries.

The results, collected in **Table 1**, show that we were able to locate all the low-energy conformers and that, while the B3 and MP2 computational models present one inversion in the relative stability order, the B2 one reproduces the reference values without any significant outlier and with an average absolute error of  $0.4 \text{ kJ mol}^{-1}$ , which is close to the typical error bar of the FPA<sup>48</sup> approach and is largely sufficient to avoid any ad hoc adjustment.

Moving to **1**, the most stable conformers for each AC choice are shown in **Figure 2** (see also Tables S1 and S2 in the SI), where it is apparent that all the most stable structures present a half-chair conformation on the ether rings. All diastereoisomers except *S-R-SS* share the same half-chair conformation with the condensed ring in equatorial position at 4a. Upon further inspection of this figure, it is evident that the *R-R-SS* diastereomer presents the substituent in 6 in a comparatively crowded pseudo-axial position, whereas the same substituent occupies an equatorial position in *R-S-SS* and *S-S-SS* diastereomers. The slight difference between *S-S-SS* and *R-S-SS* diastereomers can be ascribed to the net small attractive interaction between the O-5 lone pairs and the side chain (e.g. smaller O-5 $\cdots$ HO distance in *R-S-SS*).

**Figure 2.** Structures most stable conformer for each of diastereoisomers of  $\text{CHCl}_3$  (see text for order of chiral centers).



of the  
the four  
(**1**) in  
the

The results  
collected in **Table**  
indicate that, at all

2

computational levels and also accounting for the solvent within the PCM approximation,<sup>32</sup> the *R-S-SS* AC is the most stable. In view of the expected accuracy of B2 computations, these results rule out *R-R-SS* and *S-R-SS* diastereoisomers, but the energy difference between the other two diastereoisomers is close to the estimated error bar (about 0.5 kJ mol<sup>-1</sup>).

**Table 2.** Relative electronic energy ( $\Delta E$ ), free energy at 298 K ( $\Delta G$ ); free energy at 298 K in CDCl<sub>3</sub> solution ( $\Delta G_{PCM}$ ) values (kJ mol<sup>-1</sup>) for all diplopyrone (**1**) diastereomers calculated at the B3 and B2 levels of theory.

	B3			B2		
	$\Delta E$	$\Delta G$	$\Delta G_{PCM}$	$\Delta E$	$\Delta G$	$\Delta G_{PCM}$
<i>R-R-SS</i>	2.10	3.43	2.69	3.87	3.92	3.19
<i>R-S-SS</i>	0.00	0.00	0.00	0.00	0.00	0.00
<i>S-R-SS</i>	1.99	2.63	4.41	4.75	4.19	6.00
<i>S-S-SS</i>	0.93	0.73	0.52	0.95	0.95	0.67

3. *Comparison between experimental and simulated spectra.* As mentioned above, the proposed strategy relies on spectra predictions avoiding any empirical correction. Starting from the results obtained in the second step, we have first of all re-investigated the ECD spectra. As evident in Figure S1 in the SI, all computed ECD spectra of the four diastereoisomers are very similar to each other and always in fair agreement with experiment, thus being of no help in determining the configurations of the C-9 and C-6 centers. The results collected in Table S3 in the SI show that also optical rotation (OR) does not provide conclusive answers, although the computed values for the *R-S-SS* diastereoisomer (51.09 at the B3LYP-D3/jTZ level) are the closest to experimental values (68 in chloroform and 71 in methanol solution). As a matter of fact, while basis set, choice of the density functional, vibrational averaging and solvent effects do not alter general trends, going from a single conformer to a Boltzmann average nearly doubles the

computed value, thus casting some doubts on the robustness of the results for quantitative conclusions. For all these reasons, we resorted to vibrational spectroscopies.

The anharmonic IR and VCD spectra computed at the B3 level for the four AC choices are compared with the experimental counterparts in **Figure 3**. The comparison of experimental and computed IR spectra favors the *R-S-SS* choice based on the predicted shape of the bands at 1250 (narrow and symmetric) and 1080  $\text{cm}^{-1}$  (broader and structured). However, the computed IR spectrum of *S-S-SS* is not sufficiently different from that of *R-S-SS* to rule out the former choice without any ambiguity. On the contrary, the analysis of the VCD spectra removes any doubt: only the *R-S-SS* choice shows the peculiar quadruplet (+,+,-,+) extending from 1130 to 1050  $\text{cm}^{-1}$

1.

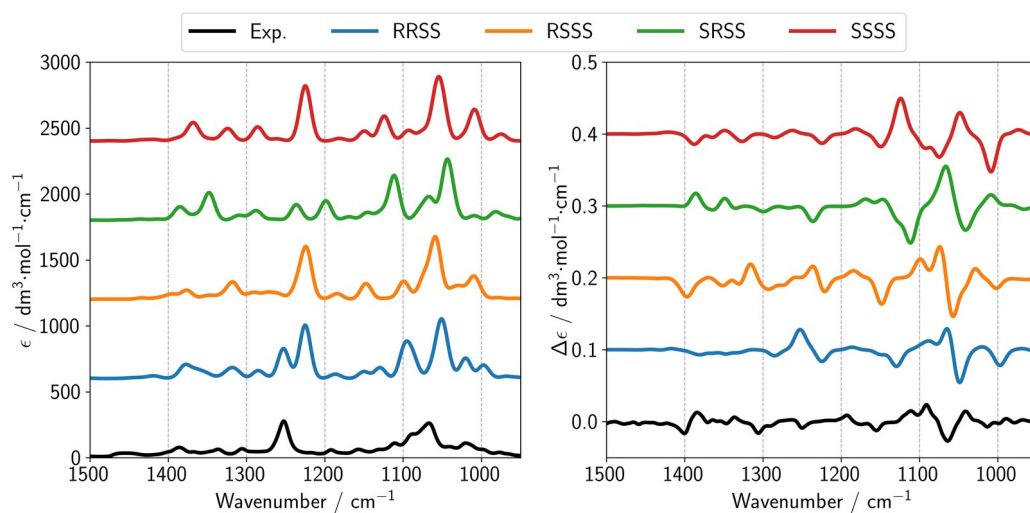


**Figure 3.** Comparison of experimental (black) IR (left) and VCD (right) spectra of diplopyrone (**1**) with the corresponding anharmonic calculated spectra (for the AC choices, see color assignment on the top-panel legend), computed at the B3 level of theory and convoluted with a Gaussian line shape with a half-width at half-height of 8  $\text{cm}^{-1}$ .

From a more quantitative point of view, the conclusions drawn in the discussion of **Figure 3** are confirmed by the similarity indexes<sup>12,13</sup> computed for the most stable conformers of the four possible diastereomers in CDCl<sub>3</sub> and reported in **Table 3**, where – for *R-S-SS* – the same indexes are also given for the B2/B3 hybrid model and for the Boltzmann-averaged spectra. The B2/B3 hybrid scheme is obtained from the B3 anharmonic force field by replacing the harmonic force constants with those at the B2 level of theory, and its remarkable accuracy and reliability are well demonstrated.<sup>7,27,44,50</sup>

Upon inspection of **Table 3**, it is quite apparent that IR spectra are not sufficient to obtain a univocal conclusion, whereas VCD spectra allow for discriminating the *R-S-SS* diastereoisomer as the most probable one. Furthermore, moving from B3 to B2/B3 results leads to an increase of the similarity indexes, which are further improved by proper consideration of Boltzmann averages of the low-lying conformers.

**Table 3.** Similarity Indexes S.I.<sup>12</sup> and Sim NN<sup>13</sup> for the comparison of computed and experimental IR and VCD spectra of the four diastereomers of diplopyrone considered in the 1500 - 950 cm<sup>-1</sup> range.

Diastereoisome r	IR		VCD	
	S.I. <sup>a</sup>	Sim NN <sup>a</sup>	S.I. <sup>a</sup>	Sim NN <sup>a</sup>
<i>R-R-SS</i>	0.71	0.50	-0.21	-0.11
<i>R-S-SS</i> <sup>b,c</sup>	0.69 (0.84) [0.84]	0.49 (0.60) [0.64]	0.32 (0.77) [0.75]	0.15 (0.48) [0.58]
<i>S-R-SS</i>	0.61	0.42	-0.52	-0.27
<i>S-S-SS</i>	0.58	0.38	0.15	0.07

<sup>a</sup> B3 anharmonic force field of the most stable conformer. <sup>b</sup> The results in parentheses have been obtained for the most stable conformer by means of the B2/B3 hybrid scheme. <sup>c</sup> The results in square brackets refer to B2/B3 computations for the Boltzmann average of 5 conformers.

In **Figure 4**, the experimental IR and VCD spectra of the *R-S-SS* diastereoisomer are compared with their anharmonic and scaled harmonic counterparts. It is noted that inclusion of anharmonicity allows for a direct comparison with experiment, with a very good agreement being obtained without the use of any scaling factor. On the other hand, in the frequency range considered in **Figure 4** (i.e. 1000-1800  $\text{cm}^{-1}$ ), scaled harmonic spectra show a good performance at the price of employing empirical, often non-general, corrections. A more detailed comparison between experiment and different levels of theory is provided in Figure S4 in the SI. In this respect, it is noteworthy that the GVPT2 approach with the incorporation of the intensity-specific test on FRs leads to a significantly improved description of the C=O stretching region, where combination bands are clearly present. However, it has to be noted that, in this region, while experimental IR spectra are reliable in all their details, the VCD signal is very weak and close to the instrumental sensitivity limit; therefore, the sign of the corresponding band cannot be taken for granted. As a matter of fact, anharmonic calculations provide weak VCD features as well. Furthermore, even if not of interest in the present investigation, the region of the XH stretchings is correctly reproduced at the GVPT2 level, whereas quite different scaling factors need to be employed for harmonic computations.

Overall, the results of **Figure 3** and **Figure 4** confirm, beyond any reasonable doubt, that the AC choice to be made is *R-S-SS*.

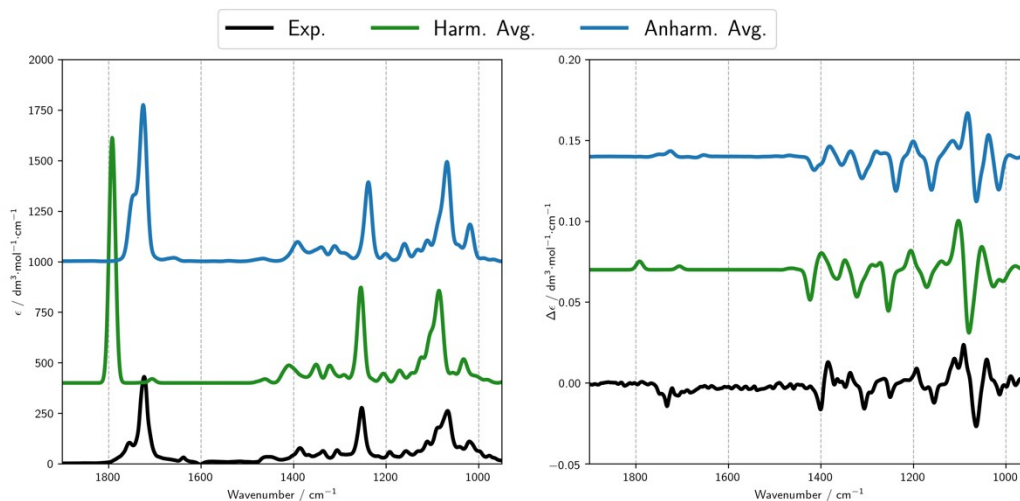


**Figure 4.** Experimental and Boltzmann-averaged (5 conformers) simulated scaled-harmonic (B3, in green) and anharmonic (B2/B3, in blue) IR (left panel) and VCD (right panel) spectra of the *R-S-SS* diastereoisomer of diplopyrone (**1**). Boltzmann averaging is based on B2 relative free energy (see Table S2 in SI), and the spectra are simulated using a Gaussian line shape with a half-width at half-height of 8  $\text{cm}^{-1}$ .

## 5. Conclusions

In conclusion, in this work it has been demonstrated that the AC of natural products or, more generally, of chiral compounds possessing multiple stereo-centers can be reliably assigned by means of an integrated strategy based on *vis-à-vis* comparisons between experimental and computed spectra, the latter including theoretical treatments that lead to noticeable improvements with respect to the most widely employed models.

General remarks deserving to be summarized, are: (i) multi-spectroscopy experimental studies can be paralleled by the corresponding computational simulations thanks to the development of user-friendly tools implementing state-of-the-art models; (ii) to define relative configurations, IR and VCD spectra can be used on equal footing as other more standard methods, like ECD and/or NMR, whenever the latter do not give solid-enough evidences; (iii) the use of VCD and IR

spectra becomes optimal in combination with a complete, rigorous high-level computational approach; (iv) a reliable yet effective treatment of anharmonicity allows for getting rid of arbitrary scaling factors in the comparison of experimental and simulated vibrational spectra, provided that the choice of the level of theory is performed with care. In this respect, the strategy introduced in this work – being developed in the framework of the VMS project – once fully implemented and standardized, will give access in a user-friendly manner to the state-of-the-art methodology above, also to non-specialists.

## ASSOCIATED CONTENT

### Supporting Information.

The Supporting Information is available free of charge on the ACS Publications website at DOI: **XXX**

Conformational search results; simulated ECD and harmonic IR and VCD spectra; anharmonic calculations and treatment of resonances and LAMS; optimized structures in XYZ format.

## AUTHOR INFORMATION

### Corresponding Authors

\*E-mail: [vincenzo.barone@sns.it](mailto:vincenzo.barone@sns.it) (Vincenzo Barone); [antonio.evidente@unina.it](mailto:antonio.evidente@unina.it) (Antonio Evidente); [sergio.abbate@unibs.it](mailto:sergio.abbate@unibs.it) (Sergio Abbate)

## ACKNOWLEDGEMENTS

The authors thank Prof. Lucia Maddau, University of Sassari, Italy for supplying the culture filtrates of *D. corticola*.

## REFERENCES

- (1) Nafie, L.A. "Vibrational Optical Activity: Principles and Applications", John Wiley & Sons, Ltd, 2011.
- (2) He, Y.; Wang, B.; Dukor, R.; Nafie, L.A. Determination of absolute configuration of chiral molecules using vibrational optical activity: a review. *Appl. Spectrosc.* **2011**, *65*, 699-723.
- (3) Polavarapu, P.L. "Optical Activity: Principles and Applications" CRC Press, Boca Raton, FL, 2017.
- (4) Abbate, S.; Burgi, L.F.; Castiglioni, E.; Lebon, F.; Longhi, G.; Toscano, E.; Caccamese, S. Assessment of configurational and conformational properties of naringenin by vibrational circular dichroism. *Chirality* **2009**, *21*, 436-441.
- (5) Aamouche, A.L.; Devlin, F.J.; Stephens, P.J. Determination of absolute configuration using circular dichroism: Tröger's Base revisited using vibrational circular dichroism. *Chem. Commun.* **1999**, 361-362.
- (6) Stephens, P.J.; Devlin, F.J.; Pan, J.J. The determination of the absolute configurations of chiral molecules using vibrational circular dichroism (VCD) spectroscopy. *Chirality*, **2008**, *20*, 643-663.
- (7) Puzzarini, C.; Bloino, J.; Tasinato, N.; Barone V. Accuracy and Interpretability: The Devil and the Holy Grail. New Routes across Old Boundaries in Computational Spectroscopy. *Chem. Rev.* **2019**, *119*, 8131-8191.
- (8) Stephens, P.J.; Devlin, F.J.; Cheeseman, J.R. "VCD Spectroscopy for Organic Chemists", CRC Press, Boca Raton, FL, 2012.

- (9) Zhao, Y.; Truhlar, D. G. Density functionals with broad applicability in chemistry. *Acc. Chem. Res.* **2008**, *41*, 157-167.
- (10) Mazzeo, G.; Cimmino, A.; Masi, M.; Longhi, G.; Maddau, L.; Memo, M.; Evidente, A.; Abbate, S. Importance and difficulties in the use of chiroptical methods to assign the absolute configuration of natural products: the case of phytotoxic pyrones and furanones produced by *diplodia corticola*. *J. Nat. Prod.* **2017**, *80*, 2406-2415.
- (11) Kuppens, T.; Langenaeker, W.; Tollenaere, J. P.; Bultinck, P. Determination of the Stereochemistry of 3-Hydroxymethyl-2,3-dihydro-[1,4]dioxino[2,3-b]-pyridine by Vibrational Circular Dichroism and the Effect of DFT Integration Grids. *J. Phys. Chem. A* **2003**, *107*, 4542-4553.
- (12) Shen, J.; Chengyue, Z.; Reiling, S.; Vaz, R. A novel computational method for comparing vibrational circular dichroism spectra. *Spectrochim. Acta A* **2010**, *76*, 418-422.
- (13) Polavarapu, P. L. "Chiroptical spectroscopy: theory and applications", CRC Press, Boca Raton, FL, 2016.
- (14) Barone, V. The Virtual Multifrequency Spectrometer: a New Paradigm for Spectroscopy. *WIREs Comp. Mol. Sci.* **2016**, *6*, 86-110.
- (15) Heshmat, M.; Nicu, V. P.; Baerends, E. J. On the Equivalence of Conformational and Enantiomeric Changes of Atomic Configuration for Vibrational Circular Dichroism Signs. *J. Phys. Chem. A* **2012**, *116*, 3454-3464.

- (16) Abbate, S.; Longhi, G.; Castiglioni, E. Near-Infrared Vibrational Circular Dichroism: VCD. Ch. 10 in “Comprehensive Chiroptical Spectroscopy”, Berova, N.; Polavarapu, P.L.; Nakanishi, K.; Woody, R.W. pp. 247-274, John Wiley & Sons, Inc., New York, 2012.
- (17) Gangemi, F.; Gangemi, R.; Longhi, G.; Abbate, S. Experimental and ab-initio calculated VCD spectra of the first OH-stretching overtone of (1R)-(-) and (1S)-(+)-endo-borneol. *Phys. Chem. Chem. Phys.* **2009**, *11*, 2683-2689.
- (18) Barone, V.; Biczysko, M.; Bloino, J. Fully anharmonic IR and Raman spectra of medium-size molecular systems: accuracy and interpretation. *Phys. Chem. Chem. Phys.* **2014**, *16*, 1759-1787.
- (19) Merten, C.; Bloino, J.; Barone, V.; Xu, Y. Anharmonicity Effects in the Vibrational CD Spectra of Propylene Oxide. *J. Phys. Chem. Lett.* **2013**, *4*, 3424-3428.
- (20) Barone, V.; Biczysko, M.; Bloino, J.; Borkowska-Panek, M.; Carnimeo, I.; Panek, P. Toward anharmonic computations of vibrational spectra for large molecular systems. *Int. J. Quantum Chem.* **2012**, *112*, 2185-2200.
- (21) Barone, V.; Baiardi, A.; Bloino, J. New developments of a multifrequency virtual spectrometer: stereo-electronic, dynamical, and environmental effects on chiroptical spectra. *Chirality* **2014**, *26*, 228-240.
- (22) Latouche, C.; Palazzetti, F.; Skouteris, D.; Barone, V. High-Accuracy Vibrational Computations for Transition-Metal Complexes Including Anharmonic Corrections: Ferrocene, Ruthenocene, and Osmocene as Test Cases. *J. Chem. Theory Comput.* **2014**, *10*, 4565-4573.

- (23) Bloino, J.; Biczysko, M.; Barone, V. Anharmonic Effects on Vibrational Spectra Intensities: Infrared, Raman, Vibrational Circular Dichroism and Raman Optical Activity. *J. Phys. Chem. A* **2015**, *119*, 11862-11874.
- (24) Bloino, J.; Biczysko, M.; Barone, V. General perturbative approach for spectroscopy, thermodynamics and kinetics: methodological background and benchmark studies. *J. Chem. Theory Comput.* **2012**, *8*, 1015-1036.
- (25) Becke, A. D., Density-functional thermochemistry. III. The role of exact exchange, *J. Chem. Phys.* **1993**, *98*, 5648-5652.
- (26) Grimme, S. Semiempirical hybrid density functional with perturbative second-order correlation. *J. Chem. Phys.* **2006**, *124*, 034108.
- (27) Biczysko, M.; Panek, M.; Scalmani, G.; Bloino, J.; Barone, V. Harmonic and anharmonic vibrational frequency calculations with the double-hybrid B2PLYP method: analytic second derivatives and benchmark studies. *J. Chem. Theory Comput.* **2010**, *6*, 2115-2125.
- (28) Grimme, S.; Ehrlich, S.; Goerigk, L. Effect of the damping function in dispersion corrected density functional theory. *J. Comput. Chem.* **2011**, *32*, 1456-1465.
- (29) Papajak, E.; Zheng, J.; Xu, X.; Leverentz, H. R.; Truhlar, D. G. Perspectives on Basis Sets Beautiful: Seasonal Plantings of Diffuse Basis Functions. *J. Chem. Theory Comput.* **2011**, *7*, 3027-3034.
- (30) Dutta, N. N.; Patkowski, K. Improving “Silver-Standard” Benchmark Interaction Energies with Bond Functions. *J. Chem. Theory Comput.* **2018**, *14*, 3053–3070.

- (31) Chandramouli, B.; Del Galdo, S.; Fusè, M.; Barone, V.; Mancini, G. Two-level stochastic search of low-energy conformers for molecular spectroscopy: implementation and validation of MM and QM models. *Phys. Chem. Chem. Phys.* **2019**, *21*, 19921-19934.
- (32) (a) Mennucci, B. Polarizable continuum model. *WIREs Comp. Mol. Sci.* **2012**, *2*, 386-404;  
(b) Cappelli, C.; Bloino, J.; Lipparini, F.; Barone, V. Toward ab-initio anharmonic vibrational circular dichroism spectra in condensed phase. *J. Phys. Chem. Lett.* **2012**, *3*, 1766-1773.
- (33) Poopari, M.; Dezhahang, Z.; Guochun, Y.; Xu, Y. Conformational Distributions of N-Acetyl-L-cysteine in Aqueous Solutions: A Combined Implicit and Explicit Solvation Treatment of VA and VCD Spectra. *Chem. Phys. Chem.* **2012**, *13*, 2310-2321.
- (34) Lipparini, F.; Egidi, F.; Cappelli, C.; Barone, V. The Optical Rotation of Methyloxirane in Aqueous Solution: A Never Ending Story? *J. Chem. Theory Comput.* **2013**, *9*, 1880-1884.
- (35) Evidente, A.; Maddau, L.; Spanu, E.; Franceschini, A.; Lazzaroni, S.; Motta, A. Diplopyrone, a New Phytotoxic Tetrahydropyranpyran-2-one Produced by *Diplodia mutila*, a Fungus Pathogen of Cork Oak. *J. Nat. Prod.* **2003**, *66*, 313-315.
- (36) Masi, M.; Maddau, L.; Linaldeddu, B. T.; Cimmino, A.; D'Amico, W.; Scanu, B.; Evidente, M.; Tuzi, A.; Evidente, A. Bioactive Secondary Metabolites Produced by the Oak Pathogen *Diplodia corticola*. *J. Agric. Food Chem.* **2016**, *64*, 217-225.
- (37) Cimmino, A.; Masi, M.; Evidente, M.; Superchi, S.; Evidente, A. Application of Mosher's method for absolute configuration assignment to bioactive plants and fungi metabolites. *J. Pharm. Biomed. Anal.* **2017**, *144*, 59-89.

- (38) Giorgio, E.; Maddau, L.; Spanu, E.; Evidente, A.; Rosini, C. Assignment of the Absolute Configuration of (+)-Diplopyrone, the Main Phytotoxin Produced by *Diplodia mutila*, the Pathogen of the Cork Oak Decline, by a Nonempirical Analysis of Its Chiroptical Properties. *J. Org. Chem.* **2005**, *70*, 7-13.
- (39) Maity S., Kanikarapu S., Marumudi K., Kunwar A. C., Yadav J. S., Mohapatra D. K. Asymmetric total synthesis of the putative structure of diplopyrone. *J. Org. Chem.* **2017**, *82*, 4561-4568.
- (40) Frisch, M. J.; Trucks, G. W.; Schlegel, H. B.; Scuseria, G. E.; Robb, M. A.; Cheeseman, J. R.; Scalmani, G.; Barone, V.; Petersson, G. A.; Nakatsuji, H.; et al., Gaussian 16 Revision C.01. 2016; Gaussian Inc. Wallingford CT.
- (41) (a) Baiardi, A.; Bloino, J.; Barone, V. Accurate simulation of resonance-Raman spectra of flexible molecules: an internal coordinates approach. *J. Chem. Theory Comput.* **2015**, *11*, 3267-3280; (b) Paoloni, L.; Rampino, S.; Barone, V. Potential energy surfaces for ring-puckering motions of flexible cyclic molecules through Cremer-Pople coordinates: computation, analysis and fitting. *J. Chem. Theory Comput.* **2019**, *15*, 4280-4294.
- (42) Halgren, T. A. MMFF VI. MMFF94s option for energy minimization studies. *J. Comput. Chem.* **1999**, *20*, 720-729.
- (43) Weigend, F.; Ahlrichs, R. Balanced basis sets of split valence, triple zeta valence and quadruple zeta valence quality for H to Rn: Design and assessment of accuracy. *Phys. Chem. Chem. Phys.* **2005**, *7*, 3297-3305.

- (44) Barone, V.; Biczysko, M.; Bloino, J.; Cimino, P.; Penocchio, E.; Puzzarini, C. CC/DFT route toward accurate structures and spectroscopic features for observed and elusive conformers of flexible molecules: pyruvic acid as a case study. *J. Chem. Theory Comput.* **2015**, *11*, 4342-4363.
- (45) Wang, J.; Spada, L.; Chen, J.; Gao, S.; Alessandrini, S.; Feng, G.; Puzzarini, C.; Gou, Q.; Grabow, J. -U.; Barone, V. The unexplored world of cycloalkene–water complexes: primary and assisting interactions unraveled by experimental and computational spectroscopy. *Angew. Chem. Int. Ed.* **2019**, DOI: 10.1002/anie.201906977.
- (46) Koenis, M. A. J.; Xia, Y.; Domingos, S. R.; Visscher, L.; Buma, W. J.; Nicu, V. P. Taming conformational heterogeneity in and with vibrational circular dichroism spectroscopy. *Chem. Sci.* **2019**, DOI: 10.1039/c9sc02866h.
- (47) He, K.; Allen, W. D. Conformers of gaseous serine. *J. Chem. Theory Comput.* **2016**, *12*, 3571-3582.
- (48) Simmonett, A. C.; Schaefer, H. F.; Allen, W. D. Enthalpy of formation and anharmonic force field of diacetylene. *J. Chem. Phys.* **2009**, *130*, 044301.
- (49) Møller, C.; Plesset, M. S. Note on an Approximation Treatment for Many-Electron Systems. *Phys. Rev.* **1934**, *46*, 618–622.
- (50) Fornaro, T.; Biczysko, M.; Barone, V. Reliable vibrational wavenumbers for C=O and N-H stretchings of isolated and hydrogen-bonded nucleic acid bases. *Phys. Chem. Chem. Phys.* **2016**, *18*, 8479-8490.